Journal of Alloys and Compounds 506 (2010) 826–830

Contents lists available at ScienceDirect

Journal of Alloys and Compounds

journal homepage: www.elsevier.com/locate/jallcom

Enhanced absorption bandwidth in carbon-coated supermalloy FeNiMo nanocapsules for a thin absorb thickness

X.G. Liu[a,b,c,*], Z.Q. Ou[c], D.Y. Geng[a,b], Z. Han[a,b], H. Wang[a,b], B. Li[a,b], E. Brück[c], Z.D. Zhang[a,b]

[a] Shenyang National Laboratory for Material Science, Institute of Metal Research, Chinese Academy of Sciences, 72 Wenhua Road, Shenyang 110016, People's Republic of China
[b] International Centre for Material Physics, Chinese Academy of Sciences, 72 Wenhua Road, Shenyang 110016, People's Republic of China
[c] Fundamental Aspects of Materials and Energy Group, Faculty of Applied Sciences, TU Delft, Mekelweg 15, 2629 JB Delft, The Netherlands

ARTICLE INFO

Article history:
Received 19 April 2010
Received in revised form 9 July 2010
Accepted 9 July 2010
Available online 16 July 2010

Keywords:
Nanocapsules
Arc-discharge
Electromagnetic wave absorption

ABSTRACT

Electromagnetic-wave absorption properties of FeNiMo/C nanocapsules with FeNiMo nanoparticles as cores and carbon as shells have been studied. The FeNiMo/C nanocapsules, synthesized by arc-discharging $Fe_{11}Ni_{79}Mo_{10}$ (at.%) alloy in ethanol, exhibited outstanding reflection loss (RL < −20 dB) in the range of 13–17.8 GHz with an absorber thickness of 1.7 mm, and an optimal RL of −64.0 dB was obtained at 13.2 GHz with an absorber thickness of 1.9 mm. The broadest bandwidth (RL < − 10 dB) from 9 to 18 GHz, covering the whole Ku-band (12.4–18 GHz) and almost the whole X-band (9–12.4 GHz), was achieved for a 2 mm layer. The excellent electromagnetic properties are ascribed to the good match between high permeability from the core of FeNiMo nanoparticles and low permittivity from the special core/shell microstructure in the FeNiMo/C nanocapsules.

1. Introduction

In recent years, with the purpose of solving the expanded electromagnetic (EM) interference problems, it is highly desirable that reflection loss (RL) exceeding −20 dB in EM-wave absorption materials, which the RL value of −20 dB corresponds to 99% EM-wave absorption, spans over a wide frequency range for a thin absorb thickness. Magnetic nanocapsules (e.g., magnetic nanoparticles coated by dielectric layers) as new type of EM-wave absorption materials has attracted interest on account of the following facts: (1) compared with the traditional ferrites, the larger saturation magnetization (M_s) leading to Snoek's limit at higher frequency. (2) The suppression of the eddy current enhancing an effective incidence to EM-wave, and (3) the combination of magnetic and dielectric materials in one nanocapsules, leading to effective interface between magnetic and dielectric materials [1–6]. Due to the interesting EM properties and the low density (~1.76 g cm^{-3}) of carbon, recent studies on nanocapsules with carbon as shells used as EM interference shielding and absorption materials have become more intensive [7–10]. Zhang and co-workers reported that carbon-coated Fe and Ni nanocapsules exhibit improved EM-wave absorption properties [1,2]. For carbon-coated Fe nanocapsules, an optimal reflection loss (RL) of −43.5 dB was reached at 9.6 GHz with an absorber thickness of 3.1 mm. The excellent EM-wave absorption properties are a consequence of a proper EM match in microstructure, a strong natural resonance, as well as multi-polarization mechanisms, etc. [2]. Han et al investigated the EM properties of FeCo/C nanocapsules [6]. In contrast to earlier reported materials, the absorption amplitude of FeCo/C nanocapsules was found not to decrease with increasing absorption-layer thickness. A RL exceeding −20 dB can be obtained for all frequencies within the 2–18 GHz range by choosing an appropriate layer thickness between 1.6 and 8.5 mm [6].

For EM-wave absorbers, the balance between complex permittivity ($\varepsilon_\gamma = \varepsilon'_\gamma - i\varepsilon''_\gamma$) and permeability ($\mu_\gamma = \mu'_\gamma - i\mu''_\gamma$) is essential in determining the reflection and attenuation properties [3–6,11–13]. The impedance match between the absorbers and free space is required to achieve low reflection and full introduction of the EM-wave into the materials. Furthermore, according to the transmission line theory, the value of permittivity (ε_γ) should be close to that of permeability (μ_γ) in order to obtain the desired impedance match. For most of magnetic metals, the values of μ'_γ are much smaller than those of ε'_γ in the microwave band, so a lower permittivity and a higher permeability are required for absorbers. Compared with microscale counterparts, nanocapsules present relatively low permittivity values due to high resistivity and enhanced permeability for the increase in effective anisotropy. It is known that Ni–Fe alloys as a kind of important soft-magnetic materials have been widely applied in the field of electronic devices and industry, in which the permalloys with nominal composi-

* Corresponding author at: Shenyang National Laboratory for Material Science, Institute of Metal Research, Chinese Academy of Sciences, 72 Wenhua Road, Shenyang 110016, People's Republic of China. Fax: +86 24 23891320.
E-mail address: liuxianguohugh@gmail.com (X.G. Liu).

0925-8388/$ – see front matter © 2010 Elsevier B.V. All rights reserved.
doi:10.1016/j.jallcom.2010.07.085

tion $Ni_{81}Fe_{19}$ (wt%) processes the highest permeability [14]. On the basis of high permeability of FeNi alloy and low permittivity of core/shell structured nanocapsules, carbon-coated FeNi alloy nanocapsules have been prepared by a modified arc-discharge technique in ethanol vapor [15]. RL exceeding −10 dB was obtained in the whole Ku-band (12.4–18 GHz) for an absorber thickness of 2.0 mm, while it exceeds −20 dB over the 13.6–16.6 GHz range. In addition, bandwidth does not change dramatically for the thicknesses of 1.87–2.1 mm for the RL values exceeding −10 dB [15]. The carbon-coated FeNi nanocapsules have improved the steadily of absorption ability.

Supermalloy $Ni_{79}Fe_{16}Mo_5$ (wt%) has an improved loss characteristic over permalloy materials, which target a higher operating frequency [14]. However, as far as we know, there has been no report on the EM properties of carbon-coated FeNiMo alloy nanocapsules. Thinking about the higher permeability of supermalloy at high frequency, it is therefore conceivable that excellent EM-wave absorption properties could be achieved in nanocapsules with a core of FeNiMo alloy nanoparticles embedded in carbon layers. The purpose of this study is to prepare the carbon-coated FeNiMo alloy nanocapsules and to investigate the EM properties of these FeNiMo/C nanocapsules. It is found that the FeNiMo/C nanocapsules prepared by arc-discharging $Fe_{11}Ni_{79}Mo_{10}$ (at.%) alloy, exhibit outstanding EM-wave absorption properties. An optimal RL of −64.0 dB was obtained at 13.2 GHz with an absorber thickness of 1.9 mm. The broadest bandwidth (RL < − 10 dB) from 9 to 18 GHz, covering the whole Ku-band (12.4–18 GHz) and almost the whole X-band (9–12.4 GHz), was obtained for a 2 mm layer. In addition, the bandwidth (RL < −20 dB) exceeds 3 GHz and the bandwidth (RL < −10 dB) exceeds 6 GHz for the absorber thicknesses of 1.5–3.0 mm.

2. Experimental

The modified arc-discharge method used in this work was described in detail elsewhere [15–17]. In brief, ingots of $Fe_{11}Ni_{79}Mo_{10}$, $Fe_{16}Ni_{79}Mo_5$ and $Fe_{14}Ni_{79}Mo_7$ (at.%) alloys served as the anode, respectively, while the cathode was a carbon needle. The atomic proportions of the ingot based on their evaporation pressures and the composition of supermalloy. The anode target was placed into a water-cooled carbon crucible. After the chamber was evacuated in a vacuum of 5.0×10^{-3} Pa, liquid ethanol of 40 ml was introduced into the chamber together with pure argon of 1.6×10^4 Pa and hydrogen of 0.4×10^4 Pa as a reactant gas and a source of hydrogen plasma. The arc-discharge current was maintained at 80 A for 2 h to evaporate alloys sufficiently. Then the products were collected from depositions on the top of the water-cooled chamber, after passivated for 8 h in argon. Three samples of the nanocapsules, prepared by arc discharging the $Fe_{11}Ni_{79}Mo_{10}$, $Fe_{16}Ni_{79}Mo_5$ and $Fe_{14}Ni_{79}Mo_7$ alloys, were denoted as samples A, B and C, respectively.

Phase analysis of the products was performed by powder X-ray diffraction (XRD) on a Rigaku D/max-2000 diffractometer at a voltage of 56 kV and a current of 182 mA with graphite monochromatized Cu-K_α ($\lambda = 0.154056$ nm) radiation. The morphology of the nanocapsules was studied in a high-resolution transmission electron microscope (HRTEM JEOL-2010) with an emission voltage of 200 kV. Quantitative analysis of the elements present in the as-prepared products was performed by means of energy dispersive spectroscopy (EDS).

For measuring the EM parameters, i.e., the complex permittivity ε_γ and permeability μ_γ, the nanocapsules were homogeneously mixed into a paraffin matrix and compressed into a cylindrical compact. First of all, paraffin wax was melted and nanocapsules were dispersed randomly into the paraffin wax with a mass ratio of 2:3. The blend was then mechanically stirred for 1 h. Finally, the nanocapsules-paraffin mixture was pressed into a toroidal cylinder with 3.04 mm in inner diameter and 7.00 mm in outer diameter for further testing. The paraffin matrix is an EM-wave transparent material, so the EM parameters obtained are mostly from the nanocapsules. The ε_γ and μ_γ of the nanocapsules-paraffin composites were determined with the transmission and reflection coaxial line method. To ensure the precision of the measurements, full two-port calibration was initially performed on the test setup to remove errors caused by the directivity, source match, load match, isolation, and frequency response in both the forward and reverse measurements [18]. In the range of 2–18 GHz, the scattering parameters (S_{11} and S_{21}) were measured by an Agilent 8722ES vector network analyzer. The ε_γ and μ_γ were determined from the scattering parameters using the Nicolson–Ross (for magnetic) and precision (for nonmagnetic) models [18,19].

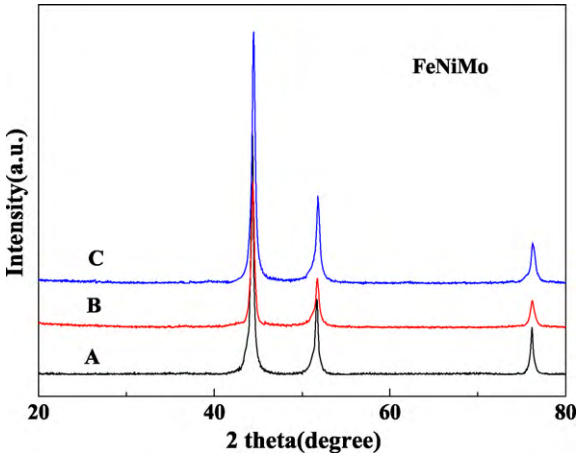

Fig. 1. XRD pattern for carbon-coated FeNiMo alloy nanocapsules of samples A–C.

3. Results and discussion

In Fig. 1, XRD patterns show the phase components of the nanocapsules (samples A–C) prepared by arc-discharging Fe–Ni–Mo alloys with different composition in ethanol vapor. All sharp reflection peaks could be indexed with the FeNi-type structure. However, they are called FeNiMo alloy nanocapsules on the basis of EDS results (Table 1) and XRD peak shift. No reflection for oxides could be found, indicating that FeNiMo nanoparticles are almost without oxidation, due to the protective carbon shell [1]. In the XRD patterns, there are no detectable peaks for pure carbon, indicating its small amount (less than 3% in the samples). Furthermore, since carbon is on the shell of the nanocapsules, it is also difficulty to detect its XRD pattern because of breaking down of the periodic boundary condition (translation symmetry) along radial direction.

The morphology of sample A can be observed clearly in Fig. 2(a). Most of the as-prepared nanocapsules are of irregular sphere shape. It is understood that the lower-energy state for the crystallization processes dominates the concrete morphology of the carbon-coated FeNiMo nanocapsules [20]. As measured from TEM observations, the size of the nanocapsules ranges from 10 to 80 nm and the average size is 32.1 nm and the shell thickness is 4.5 nm for sample A. The HRTEM image, as shown in Fig. 2(b), clearly indicates that a nanocapsule owns a 'core/shell' type structure and the inner FeNiMo alloy cores are encapsulated into the onion-like carbon cages. The lattice plane spacing of the coating layers is about 0.34 nm, which corresponds to the (0 0 2) plane of graphite. Nevertheless, a lot of lattice imperfections can be seen in the outer

Table 1
Composition of FeNiMo/C nanocapsules and master alloys, the size distribution and average diameter/shell thickness of FeNiMo/C nanocapsules.

Sample	Master alloys (at.%)			Nanocapsules size distribution (nm)	Average diameter/shell thickness (nm)	Nanocapsules (at.%)			
	Fe	Ni	Mo			Fe	Ni	Mo	C
A	11	79	10	10–80	32.1/4.5	11.8	53.6	3.3	31.3
B	16	79	5	10–80	35.5/3.1	13.5	52.4	1.5	32.5
C	14	79	7	10–80	34.2/3.9	13.0	53.1	2.2	31.7

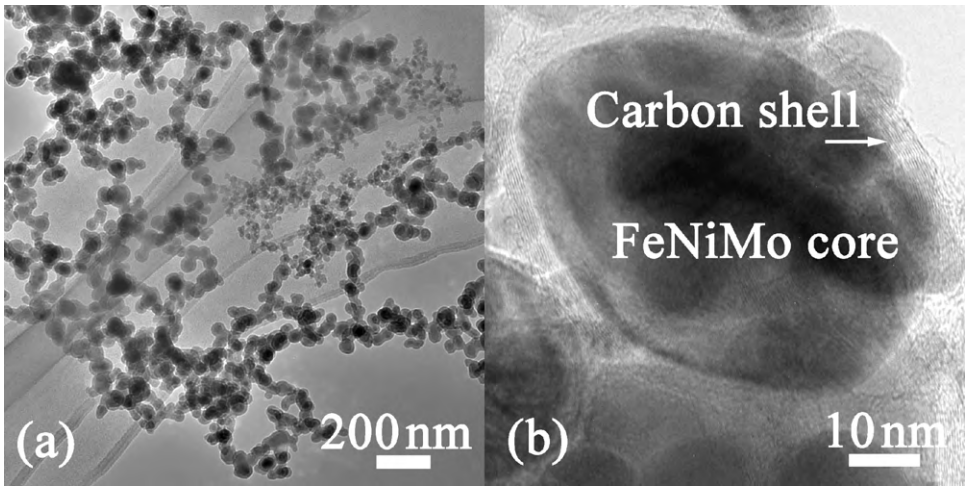

Fig. 2. (a) TEM and (b) HRTEM images of carbon-coated FeNiMo nanocapsules of sample A.

shells as a consequence of the serious bending and collapsing of the graphite atom layer, which is similar with the Fe/C and FeNi/C nanocapsules [1,15]. In addition, the graphite shell of the carbon-coated FeNiMo nanocapsules prepared in ethanol vapor is thinner than that of Fe/C and Ni/C nanocapsules prepared in CH_4, which is ascribed to the lower carbon content in ethanol [15,16].

The particle size distribution, average diameter, shell thickness and composition of the FeNiMo/C nanocapsules (samples A–C), as measured from TEM observation and EDS results and the composition of their master alloys, are presented in Table 1. In Table 1, the difference between the compositions of the starting FeNiMo alloys and the as-prepared nanocapsules is displayed. This difference can be ascribed to the formation mechanism of the nanocapsules, i.e., different evaporating pressures, melting points for iron, nickel and molybdenum atoms, during the arc-discharging process. For an evaporating pressure of 133 Pa (1 Torr), the corresponding evaporating temperatures are 1537 °C for Fe, 1907 °C for Ni and 3117 °C for Mo. The melting points of iron, nickel and molybdenum are 1495, 1453 and 2617 °C, respectively. In the arc-discharge process, mainly iron and nickel atoms will evaporate and then collide in the gas phase to condenses first to the solid state, but a small amount of molybdenum atoms evaporate into the FeNi phase as solid-solution atoms [20]. The decomposition of ethanol vapor, due to the high temperature in the arc-discharge process, provides sufficient carbon atoms to form carbon shells on the surface of FeNiMo nanoparticles during the solidification process. Combining with the atomic proportions measured by EDS and atomic weight, it is noted that the composition of nanocapsules in sample A is very close to the supermalloy $Ni_{79}Fe_{16}Mo_5$. It is observed that the samples A–C process the same size distribution of nanocapsules, due to the same experimental parameters during the arc-discharge process. The difference in the average diameter and shell thickness is ascribed to the evaporation of different elements and the sorption of nanoparticles with different size during the arc-discharge. Since the EM properties of the nanoparticles essentially depend on their size and especially on the core/shell proportion [1–7], the different particle size and shell thickness indicate different EM-absorptive properties in samples A–C.

Fig. 3 shows the frequency dependence of ε_γ and μ_γ of nanocapsules-paraffin composites. As seen in Fig. 3(a), there is a similar tendency of the real part (ε_r') and the imaginary part (ε_r'') of ε_γ in samples A–C, due to the similar microstructure in nanocapsules. The values of ε_r' decreases with increasing frequency in the 2–18 GHz range, while the values of ε_r'' exhibit a significant fluctuation, over the 2–18 GHz range, ascribed to the displacement current lag at the 'core/shell' interface [2]. Compared with the microscale metal-particles composites (for α-Fe particles, $\varepsilon_r' = 230$ and $\varepsilon_r'' = 400$) [21], the present nanocapsules have much lower permittivity, indicating a higher resistance. This is ascribed to the following fact: the graphite layers, in which the electrical resistivity

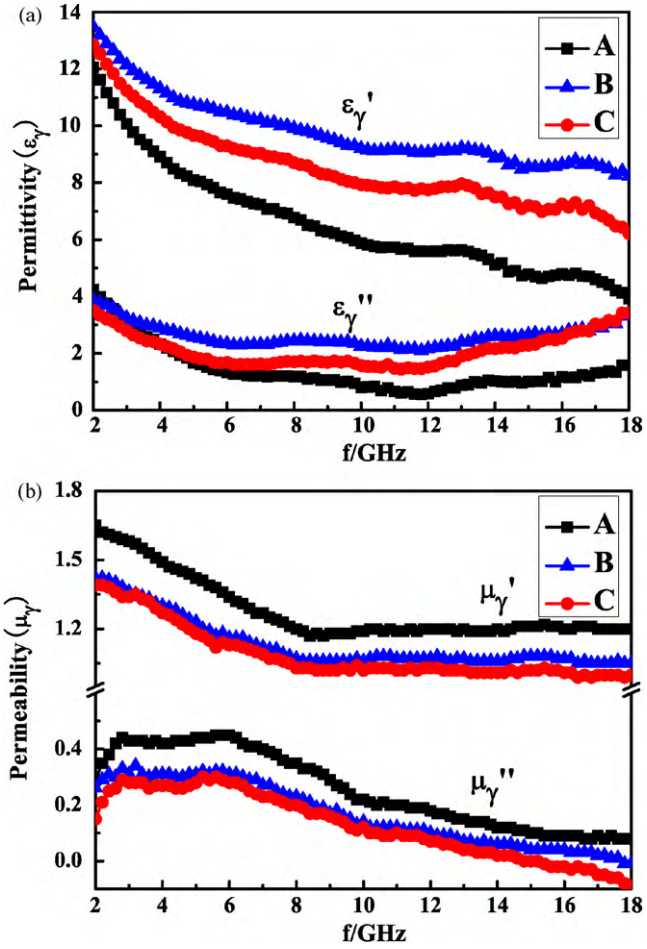

Fig. 3. (a) Relative permittivity and (b) relative permeability of FeNiMo nanocapsules-paraffin composite as a function of frequency.

is increased from the special microstructure and defect properties when thickness is in several nanometres, block the formation of an electric conducting network, which can contribute to low polarization and dielectric loss [18]. However, the differences in the permittivity values of samples A–C in the whole 2–18 GHz range indicate a higher electrical resistivity of the samples A, which comes from the smaller particles' sizes and thicker shell. In general, a high electrical resistivity is good for improving the EM-wave absorption properties.

The real part (μ_r') and the imaginary part (μ_r'') of μ_γ for samples A–C show almost the same variation in the 2–18 GHz range. μ_r' values decrease with frequency in the 2–9 GHz range and retain almost constant from 9 to18 GHz, while μ_r'' exhibit broad multi-resonance peaks at about 2–9 GHz, which implies that natural-resonance occurs in the FeNiMo/C nanocapsules. It can be speculated that the multi-resonance peaks, as shown in Fig. 3(b), are a consequence of the small size effect, surface effect and spin wave excitations, which have been defined as 'exchange mode' resonance [22,23]. Compared with the bulk FeNiMo, the natural-resonance frequency (f_r) of the FeNiMo nanoparticles has been remarkably shifted to higher frequency, which is ascribed to the considerable increase of the surface anisotropy field (H_{eff}) due to the size effect. These multi-resonance phenomena have also been analyzed in detail in recent investigation [2–6]. The similar variation in μ_r' and μ_r'' arises from the same size distribution and similar average diameter and shell thickness for samples A–C. Compared with samples B and C, sample A processes higher values of μ_r' and μ_r'', which can be explained by the fact that the composition of nanocapsules is very close to that of the supermalloy, leading to high μ_r in the GHz range.

Generally, excellent EM-wave absorption results from efficient complementarities between the relative permittivity and permeability in materials [3–5]. To further prove the EM-wave absorption properties, the RL values of composites with different absorptive thicknesses were calculated in the range of 2–18 GHz, as shown in Fig. 4, according to the transmit-line theory, by using the experimental data of relative complex permeability and permittivity [15,16]. The RL of EM-absorptive materials measured in decibel (dB) greater than −20 dB (note that −20 dB corresponds to 99% EM-wave absorption), should be adequate. From the view of applications, the absorbing ability (e.g., wide frequency range, strong absorption, etc.) must be improved for EM-wave absorbers, in which the upper limit of absorbing thickness is selected as 3 mm. As shown in Fig. 4(a), an optimal RL of −64.0 dB was obtained at 13.2 GHz with an absorber thickness of 1.9 mm. For the absorber thickness of 1.7 mm, the broadest bandwidth (RL < −20 dB) is achieved in the range of 13–17.8 GHz that is broader than that reported previously for a single thickness [1–15]. The broadest bandwidth for RL < − 10 dB (note that −10 dB corresponds to about 70% EM-wave absorption) from 9 to 18 GHz, covering the whole Ku-band (12.4–18 GHz) and almost the whole X-band (9–12.4 GHz), was obtained for a 2 mm layer. In addition, the bandwidth (RL < −20 dB) exceeds 3 GHz and the bandwidth (RL < −10 dB) exceeds 6 GHz for the absorber thicknesses of 1.5–3.0 mm. Compared with samples B and C, the sample A exhibits larger optimal RL value, broader bandwidth (for both RL < −20 dB and RL < −10 dB). According to the transmission line theory, as the value of permittivity is close to that of permeability, one can obtain the desired impedance match. Compared with samples B and C, the sample A presents a lower permittivity and higher permeability. The smaller average size and thicker shell lead to lower polarization and dielectric loss, which make permittivity low. The composition of FeNiMo cores is very close to the composition of supermalloy, which leads to a higher permeability at the GHz range. The excellent EM-absorptive properties of the sample A come from the good match between high permeability from the FeNiMo nanoparticles and low permittivity from the special core/shell microstructure in the FeNiMo/C nanocapsules.

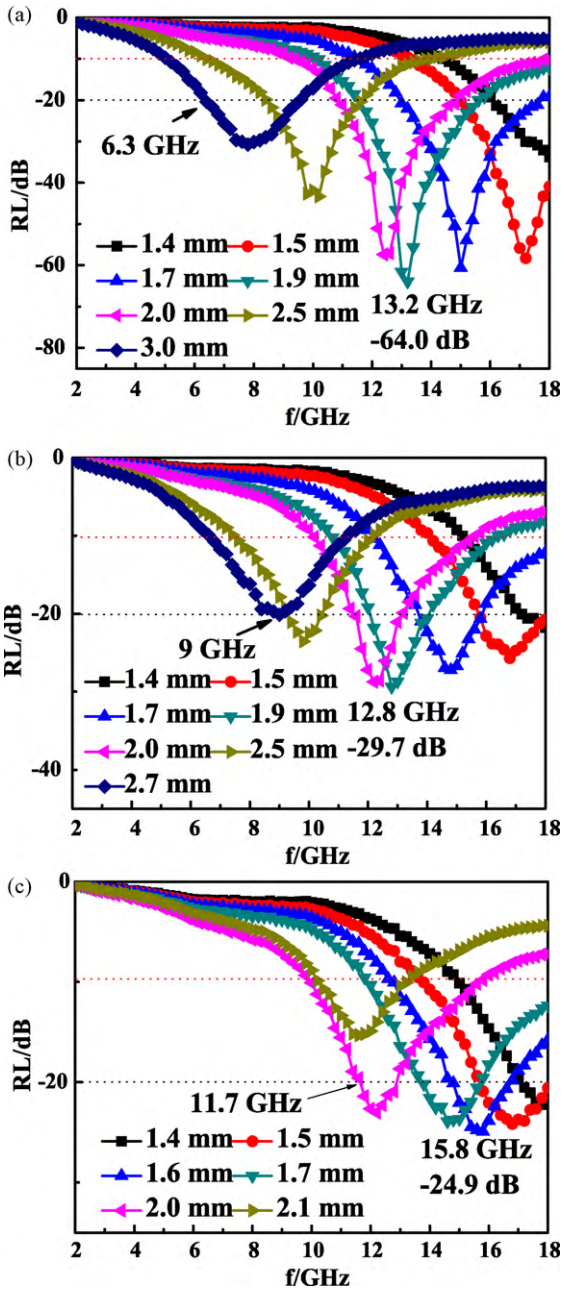

Fig. 4. Frequency dependence of RL of composites of paraffin and (a) sample A, (b) sample B and (c) sample C, for varying thickness of the absorbent.

4. Conclusion

In summary, the carbon-coated FeNiMo nanocapsules have been prepared by the arc-discharge technique in ethanol vapor. The phase, composition and microstructure of the FeNiMo/C nanocapsules have been investigated by means of XRD, EDS and HRTEM. The FeNiMo/C nanocapsules own a 'core/shell' type structure and the inner FeNiMo alloy nanoparticles as cores are encapsulated into the onion-like carbon cages as shells. The composition of as-prepared FeNiMo/C nanocapsules by arc-discharging $Fe_{11}Ni_{79}Mo_{10}$ (at.%) is very close to the supermalloy $Ni_{79}Fe_{16}Mo_5$, which leads to the high permeability at the GHz range. The special core/shell microstructure in the nanocapsules results in the low permittivity.

The good match between high permeability and low permittivity result in outstanding EM-wave absorption properties of FeNiMo/C nanocapsules. An optimal RL of −64.0 dB was obtained at 13.2 GHz with an absorber thickness of 1.9 mm. For the absorber thickness of 1.7 mm, the bandwidth (RL < −20 dB) is achieved in the range of 13–17.8 GHz that is broader than that reported previously for a single thickness. The broadest bandwidth (RL < − 10 dB) from 9 to 18 GHz, covering the whole Ku-band and almost the whole X-band, was obtained for a 2 mm layer. In addition, the bandwidth (RL < −20 dB) exceeds 3 GHz and the bandwidth (RL < −10 dB) exceeds 6 GHz for any absorber thicknesses in the range of 1.5–3.0 mm. The results suggest that the FeNiMo/C nanocapsules with wide bandwidth absorption are excellent EM-wave absorption materials.

Acknowledgments

This work has been supported partly by the Scientific Exchange Program between China and the Netherlands, partly by the National Basic Research Program (No. 2010CB934603) of China, Ministry of Science and Technology of China, and partly by the National Natural Science Foundation of China under Grant No. 50831006 and 50701045.

References

[1] X.F. Zhang, X.L. Dong, H. Huang, Y.Y. Liu, W.N. Wang, X.G. Zhu, B. Lv, J.P. Lei, C.G. Lee, Appl. Phys. Lett. 89 (2006) 053115.
[2] X.F. Zhang, X.L. Dong, H. Huang, Y.Y. Liu, B. Lv, J.P. Lei, C.J. Choi, J. Phys. D: Appl. Phys. 40 (2007) 5383–5387.
[3] X.G. Liu, D.Y. Geng, H. Meng, P.J. Shang, Z.D. Zhang, Appl. Phys. Lett. 92 (2008) 173117.
[4] X.G. Liu, D.Y. Geng, Z.D. Zhang, Appl. Phys. Lett. 92 (2008) 243110.
[5] X.G. Liu, J.J. Jiang, D.Y. Geng, Z. Han, W. Liu, Z.D. Zhang, Appl. Phys. Lett. 94 (2009) 053119.
[6] Z. Han, D. Li, H. Wang, X.G. Liu, J. Li, D.Y. Geng, Z.D. Zhang, Appl. Phys. Lett. 95 (2009) 023114.
[7] J.R. Liu, M. Itoh, T. Horikawa, M. Itakura, N. Kuwano, K. Machida, J. Phys. D: Appl. Phys. 37 (2004) 2737–2741.
[8] R.C. Che, L.M. Peng, X.F. Duan, Q. Chen, X.L. Liang, Adv. Mater. 16 (2004) 401–405.
[9] A. Wadhawan, D. Garrett, J.M. Perez, Appl. Phys. Lett. 83 (2003) 2683–2685.
[10] R.T. Lv, F.Y. Kang, J.L. Gu, X.C. Gui, J.Q. Wei, K.L. Wang, D.H. Wu, Appl. Phys. Lett. 93 (2008) 223105.
[11] J. Ma, J.G. Li, X. Ni, X.D. Zhang, J.J. Huang, Appl. Phys. Lett. 95 (2009) 102505.
[12] Y.J. Chen, P. Gao, C.L. Zhu, R.X. Wang, L.J. Wang, M.S. Cao, X.Y. Fang, J. Appl. Phys. 106 (2009) 054303.
[13] X.L. Shi, M.S. Cao, J. Yuan, X.Y. Fang, Appl. Phys. Lett. 95 (2009) 163108.
[14] J. Füzer, P. Kollár, D. Olekšáková, S. Roth, J. Alloy Compd. 483 (2009) 557–559.
[15] X.G. Liu, B. Li, D.Y. Geng, F. Yang, Z.D. Zhang, Carbon 47 (2009) 470–474.
[16] X.G. Liu, Z.Q. Ou, D.Y. Geng, Z. Han, Z.G. Xie, Z.D. Zhang, J. Phys. D: Appl. Phys. 42 (2009) 155004.
[17] X.G. Liu, D.Y. Geng, Q. Zhang, J.J. Jiang, W. Liu, Z.D. Zhang, Appl. Phys. Lett. 94 (2009) 103104.
[18] B. Lu, H. Huang, X.L. Dong, X.F. Zhang, J.P. Lei, J.P. Sun, C. Dong, J. Appl. Phys. 104 (2008) 114313.
[19] A.N. Yusoff, M.H. Abdullah, S.H. Ahmad, S.F. Jusoh, A.A. Manso, S.A.A. Hamid, J. Appl. Phys. 92 (2002) 876–882.
[20] D.Y. Geng, Z.D. Zhang, W.S. Zhang, P.Z. Si, X.G. Zhao, W. Liu, K.Y. Hu, Z.X. Jin, X.P. Song, Scr. Mater. 48 (2003) 593–598.
[21] S.S. Kim, S.T. Kim, Y.C. Yoon, K.S. Lee, J. Appl. Phys. 97 (2005), 10F905.
[22] D. Mercier, J.C.S. Lévy, G. Viau, F.F. Vincent, F. Fiévet, P. Toneguzzo, O. Acher, Phys. Rev. B 62 (2000) 532–544.
[23] A. Aharoni, J. Appl. Phys. 81 (1997) 830–833.